Transactions on Engineering Sciences vol 12, © 1996 WIT Press, www.witpress.com, ISSN 1743-3533

# Numerical simulation of a 2D crystal growth problem: latent heat effects and solid-liquid interface morphology

D. Morvan, M. El Ganaoui, J. Ouazzani, P. Bontoux
*Institut de Recherche sur les Phénomenès Hors Équilibre, UMR 138, CNRS Universités D'Aix-Marseille 1&2, IMT Technopôle de Château Gombert, 13451 Marseille cedex 20, France*

## Abstract

The influence of latent heat and natural convection in the melt and the shape of the melt–crystal interface are analyzed for a vertical Bridgman crystal growth system by direct numerical simulation. The temperature and the velocity field in the melt and in the crystal are computed using an homogenization technique. Initially the ampoule contains poly–crystal material, these container is translated inside a furnace which includes two heating zones characterized by two temperatures which are respectively greater and lower than the melted temperature of the material. The two heating zones in the furnace are separated by an adiabatic zone when the solid–liquid phase change occur. The control of the solidification conditions (phase change front velocity, gravity ...) permits to produce with these technique very high quality single crystals. The results presented in this paper show the effects of various gravitational conditions upon the flow in the melted part of the material inside the ampoule. We have also analyzed the effect of the latent heat upon the shape of the melt–crystal interface and the convective cells in the melted pool.

## 1 Introduction

The recent progresses registered in electronics industry are due essentially to the improvements of the fabrication process of electronics components. The improvement of the quality of semiconductors single–crystals which constitute the basic material of electronics components, has permitted to reduce the size of these components and therefore to increase the integration density and the performance of each new generation of products. This fabrication is performed using various techniques of crystal growth which can be separated in two classes:

- confined crystal growth technique (vertical Bridgman–Stockbarger, gradient freeze methods) which consists to load the initially poly–crystal material inside an ampoule, then to realize a melting and a resolidification at low velocity to produce a transformation of this material to a single crystal rod.

- meniscus–defined (Czochralski, floating zone methods), which consists to realize this transformation in a system which includes also a free surface, the stress induce inside the material are less important than in the previous method because of the free surface which permits the expansion of the material during the heat loading.

Confined melt growth systems are considered to be more interesting because they permit to produce in better conditions, exotic alloy materials with an accurate control of the stoichiometry.
The development of the next generation of electronics components needs to increase the single–crystal rod diameter, but experiments and numerical studies have shown that in the same way the convective motions which develop inside the melt could be also amplified with a significant action upon the crystal growth. To reduce these convective transport phenomena, the first possibility is to place the growth system in microgravity conditions. Actually the microgravity technologies are limited to laboratory experiments, the flying opportunities (space lab, rocket ...) are exceptional, therefore the preparation of optimal experimental conditions is very important and the numerical simulations of such process can represents a adapted tool for the definition of these conditions.
The results presented in this paper, constitute a part of a numerical study that we have performed for the resolution of heat and mass transfer inside a crystal growth ampoule during a resolidification operation using a Bridgman–Stockbarger technique. The calculation of various variables (enthalpy, velocity ...) which characterize the physical behaviour of this system is performed using homogenization technique. These method consists to represent the solid–liquid mixture as a single continuum medium defined after average operations performed for each species and each phases present in the system [1, 2]. The main advantage of these method is its ability to solve fusion–solidification problems of both pure and alloy materials. It is not necessary for the mesh to follow the movements and the deformations of the melt–crystal interface. Therefore it is possible to solve problems which does not exhibit smooth phase front as those encountered during dendritic growth. Various experimental conditions have been tested to study the effects of the gravity acceleration and the relative magnitude of the latent heat compared to the maximum temperature gap induced by the heating plots inside the furnace. A particular attention has been observed concerning the influence of these physical parameter to the deformation and the motions of the crystal–melt interface.

# 2 Mathematical formulation

The geometry of the computational domain is rectangular with a length/width shape ratio equal to 10. The problem is solved in a fixed referential with regard to the ampoule, therefore the cooling induced by the furnace is represented with a time dependent temperature profile along the lateral boundary of the ampoule characterized with a scanning velocity $U_s$. The temperature profile along lateral boundary is composed by two isothermal zones (hot temperature $T_1$ and cold temperature $T_0$) linked by an adiabatic plug zone with a width equal to 2 times the ampoule diameter (Figure 1) and animated with a constant translation velocity $U_s$. In order to reduce the number of physical parameters, the variables which describe the state of the system are reduced to dimensionless form using the following reference scales:

- length: crystal diameter $d$
- temperature (maximum temperature variation in the furnace): $\Delta T = T_1 - T_0$
- density, specific and conductivity: $\rho_l$, $c_s$ and $k_l$
- velocity: $U = k_l \Delta T / \rho c_s d$
- enthalpy: $c_s \Delta T$

The dimensionless variables defined from these reference scales are:

$$\widetilde{x_i} = \frac{x_i}{d} \quad \widetilde{t} = \frac{tU}{d} \quad \widetilde{v_i} = \frac{v_i}{U} \tag{1}$$

$$\widetilde{T} = \frac{T}{\Delta T} \quad \widetilde{h} = \frac{h}{c_s \Delta T} \quad \widetilde{p} = \frac{p}{\rho U^2} \tag{2}$$

$$\widetilde{k} = \frac{k}{k_l} \quad \widetilde{c_\phi} = \frac{c_\phi}{c_s} \quad \widetilde{\rho} = \frac{\rho}{\rho_l} \tag{3}$$

With these definitions the dimensionless enthalpies for the solid and the liquid phase can be written as follows:

$$\widetilde{h_s} = \widetilde{T} \tag{4}$$

$$\widetilde{h_l} = \widetilde{c_l}\widetilde{T} + (1 - \widetilde{c_l})\widetilde{T_f} + \frac{1}{Ste} \tag{5}$$

With these reference scales and if we assume that the density variations with temperature is reduced to the buoyancy forces (Boussinesq approximation), the set of transport equations which control the physical behaviour of this system, can be written as follows:

$$\frac{\partial}{\partial \widetilde{x_j}} (\widetilde{v_j}) = 0 \tag{6}$$

$$\frac{\partial}{\partial \widetilde{t}}(\widetilde{\rho}\widetilde{v}_i) + \frac{\partial}{\partial \widetilde{x}_j}(\widetilde{\rho v_j}\widetilde{v}_i) = -\frac{\partial \widetilde{p}}{\partial \widetilde{x}_i} + Pr\frac{\partial}{\partial \widetilde{x}_j}\left(\widetilde{\rho}\frac{\partial \widetilde{v}_i}{\partial \widetilde{x}_j}\right) + RaPr\frac{g_i}{g}\widetilde{T} - \frac{Prd^2}{K}\widetilde{\rho}\left(\widetilde{v}_i - \widetilde{v}_i^s\right) \quad (7)$$

$$\frac{\partial}{\partial \widetilde{t}}\left(\widetilde{\rho}\widetilde{h}\right) + \frac{\partial}{\partial \widetilde{x}_j}\left(\widetilde{\rho v_j}\widetilde{h}\right) = \frac{\partial}{\partial \widetilde{x}_j}\left(\widetilde{k}\frac{\partial \widetilde{h}_s}{\partial \widetilde{x}_j}\right) - \frac{\partial}{\partial \widetilde{x}_j}\left(\widetilde{\rho}\left(\widetilde{h}_l - \widetilde{h}\right)\left(\widetilde{v_j} - \widetilde{v_j^s}\right)\right) \quad (8)$$

The dimensionless physical parameters which appear in equations (6–8) are defined as follows:

$$\text{Rayleigh number: } Ra = \frac{g\beta c_s \Delta T \rho^2 d^3}{k\mu} \quad (9)$$

$$\text{Prandtl number: } Pr = \frac{\mu c_s}{k} \quad (10)$$

$$\text{Stefan number: } Ste = \frac{c_s \Delta T}{h_f} \quad (11)$$

$$\text{Peclet number: } Pe = \frac{U_s}{U} \quad (12)$$

$$\text{crystal growth (scanning) velocity: } U_s \quad (13)$$

The calculations have been performed for a 28 × 200 mesh grid. Previous numerical results [3] have shown that a boundary layer regime can develop along the vertical walls of the ampoule when the convective transport increase in the melt (induced for example by an augmentation of the gravity magnitude). Therefore to obtain an adequate accuracy for the numerical resolution inside this boundary layer region, it is necessary to refine the mesh along the vertical boundaries.
The numerical integration is performed using a finite volume method. The time integration scheme is a first order implicit Euler scheme and the spatial integration is performed using a ULTRA-QUICK scheme [4], which represents a good compromise between accuracy and simplicity.

# 3 Numerical results

The tested values for the dimensionless physical parameters are evaluated from experimental conditions of a crystal growth operation for a semiconductor material such as gallium-doped germanium (Ga–Ge) [5], (no variations of the density, the conductivity and the specific heat are introduced with the solid–liquid phase change):

- Rayleigh number: $10^4$.
- Prandtl number: $10^{-2}$.

- Peclet number: $510^{-3}$.
- Stefan number: from 0.1 to $\infty$ ($Ste^{-1} = 0, 5, 10$).

The solid–liquid phase change is assumed to occur between a solidus ($T_s$) and a liquidus ($T_l$) temperature equal to 0.4 and 0.6 (dimensionless values). The numerical results presented on Figures 2 to 4 show the velocity vectors fields obtained for 3 values of the the Stefan number ($Ste^{-1} = 0, 5, 10$) at different times during a crystal growth operation. The results obtained for $Ste^{-1} = 0$ (for which the latent heat effects are neglected) show that the flow pattern in the melt is symmetrical and is composed during the major part of the process of four contra–rotative vortices. For this Stefan number the solution exhibits a flat crystal–melt interface (represented by the solidus isothermal curve) (see Figure 2). If the latent heat effects are taken into account, the crystal–melt interface is distorted and becomes convex towards the liquid phase (see Figures 3, 4). In fact the inertia caused during the melting phase by the augmentation of the latent heat, induces a delay for the growth of the solid phase. From hydrodynamics point of view, the increase of latent heat effects appears by an augmentation of eddy activity near the phase change region, with the addition of two ($Ste^{-1} = 5$) (Figure 3) then four ($Ste^{-1} = 10$) (Figure 4) supplementary vortices. During the third part of the process (at the end of the solidification phase) the reduction of the longitudinal melt dimension begins to affect the vortex intensity at the top of the ampoule. Before this time the longitudinal dimension does not seem to have an influence upon the flow pattern and its intensity. The same behaviour has been found with previous numerical study for a cylindrical configuration [6].This results permits to validate a common assumption used for many numerical simulation of Bridgman crystal growth process: the equivalence to study this crystal growth problem in a fixed referential or in a referential moving with the crystal–melt interface [7, 3, 5, 8, 9]. Excepting at the end of the solidification, the melt flow near the crystal–melt interface (which represents the most important contribution for the crystal growth process) is not affected by the continuous reduction of the melt region.

A solid–liquid interface which is convex towards the liquid phase (as observed on these numerical results) results from the differences between boundary conditions imposed along the wall and the axis of the ampoule. The boundary condition imposed at the axis is less constrained than those imposed along the wall, which permits a greater freedom for the positioning of the solidification front. In fact for $Ste^{-1} = 5$ and 10 the melt–crystal position along the wall of the ampoule is situated close to the lower bound of the adiabatic zone. Because of the temperature fixed under this position, the solid–liquid interface could not overshoot this limit, which explain why the deformation of this interface is more important near the axis of the ampoule. Therefore to reduce the deformation of the solidification front with

high latent heat to sensitive heat ratio represented by $Ste^{-1}$, it is necessary to increase the length of the adiabatic zone between the two isothermal (cold and hot temperatures) regions.

# 4 Conclusion

A finite volume discretization modelling using homogenization technique has been presented for the resolution of a crystal growth problem. Computational results have shown that this approach could correctly treat such solidification problem without needing the continual remeshing of the domain to follow the movements of the fusion–solidification front. They have also shown a great influence of the latent heat upon the shape of the phase–change front and the flow of the melted material in this region. The gravity magnitude represented by the Rayleigh number seems to have no effect upon the shape and the propagation of the melt–crystal front. The deformation of this phase–change interface seems to be essentially affected by the latent heat to sensible heat ratio and the dimension of the adiabatic zone along the wall of the ampoule.
Before their generalization these results must be confirmed for larger selection of the physical parameters, for example for larger values of the crystal growth velocity represented by the Peclet number and other configuration of temperature boundary conditions along the lateral face of the ampoule, which permit for example to take into account the thermal properties of the ampoule wall.

# References

[1] W.D. Bennon and F.P. Incropera. A continuum model for momentum, heat and species transport in binary solid-liquid phase change systems: 1 model formulation. *Int. J. Heat Mass Transfer*, 30(10):2161–2170, 1987.

[2] W.D. Bennon and F.P. Incropera. A continuum model for momentum, heat and species transport in binary solid-liquid phase change systems: 2 application to solidification in a rectangular cavity. *Int. J. Heat Mass Transfer*, 30(10):2171–2187, 1987.

[3] P.M. Adornato and R.A. Brown. Convection and segregation in directional solidification of dilute and non–dilute binary alloys: effects of ampoule and furnace design. *J. Crystal Growth*, 80:155–190, 1987.

[4] B.P. Leonard. The ultimate conservative difference scheme applied to unsteady one–dimensional advection. *Comput. Methods Appl. Mech. Engineering*, 88:17–74, 1991.

[5] J. Chang and R.A. Brown. Radial segregation induced by natural convection and melt–solid interface shape in vertical bridgman growth. *J. Crystal Growth*, 63:343–364, 1983.

[6] R.A. Brown and Do Hyum Kim. Modelling of directional solidification: from scheil to detailed numerical simulation. *J. Crystal Growth*, 109:50–65, 1991.

[7] R.A. Brown. Theory of transport processes in single crystal growth from the melt. *AIChE Journal*, 34(6):881–911, 1988.

[8] Y. Zhang, J.I.D. Alexander, and J. Ouazzani. A chebyshev collocation method for moving boundaries, heat transfer, and convection during directional solidification. *Int. J. Num. Meth. Heat Fluid Flow*, 4:115–129, 1994.

[9] Ph. Larroude, J. Ouazzani, J. Alexander, and P. Bontoux. Symmetry breaking flow transition and oscillatory flows in 2d directional solidification model. *Eur. J. Mech. B–Fluids*, 13(3):353–381, 1994.

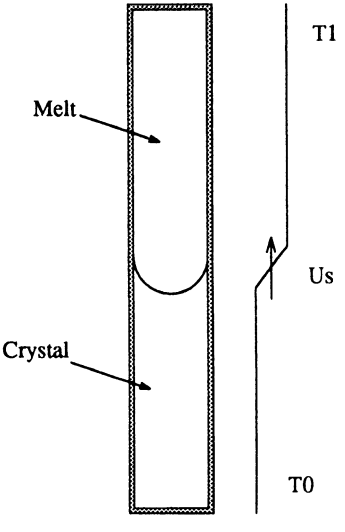


Figure 1: Bridgman–Stockbarger crystal growth technique (ampoule geometry and temperature boundary conditions).

Figure 2: Flow pattern in the melt during a crystal growth process for $Ra = 10^4$ and $Ste^{-1} = 0$ ($U_{max} = 0.5$).

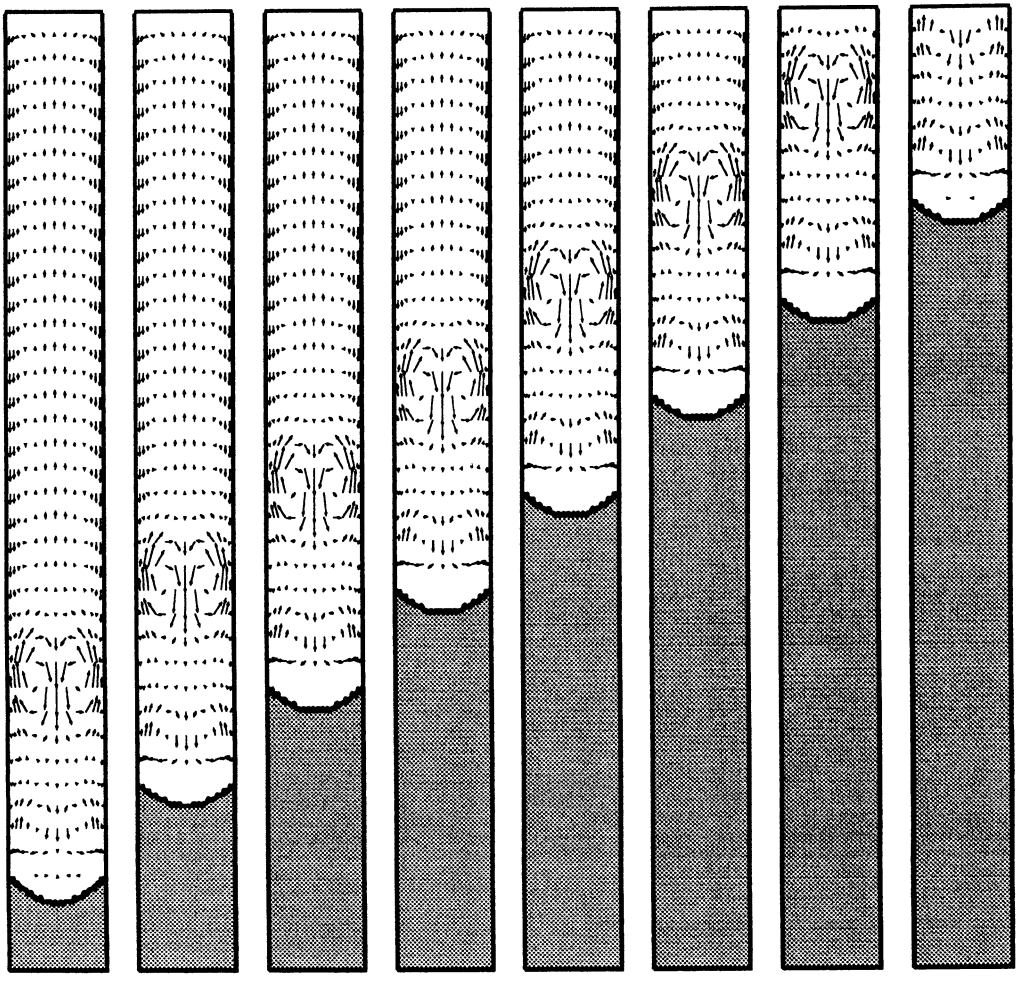

Figure 3: Flow pattern in the melt during a crystal growth process for $Ra = 10^4$ and $Ste^{-1} = 5$ ($U_{max} = 0.5$).

Figure 4: Flow pattern in the melt during a crystal growth process for $Ra = 10^4$ and $Ste^{-1} = 10$ ($U_{max} = 0.5$).